British Journal of Pharmacology (1997) 121, 617–624

Comparative direct electrophysiological effects of propofol on the conduction system and ionic channels of rabbit hearts

[1]Mei-Hwan Wu, *Ming-Jai Su & Selma Siu-Mun Sun

Department of Pediatrics and *Pharmacology, Medical College, National Taiwan University, Taipei, Taiwan

1 Propofol, an intravenous anaesthetic agent, can affect cardiac conduction but the ionic mechanisms have not been well defined.

2 This study measured the direct effects of propofol on the cardiac conduction system by using intracardiac recording/stimulation in Langendorff-perfused rabbit hearts. The underlying ionic mechanism was elucidated by using the whole-cell voltage clamp on rabbit isolated atrial and ventricular myocytes.

3 Propofol prolonged significantly the AV conduction (AH) interval at a clinically relevant concentration (3 μM). This AH interval prolongation was dose-dependent (3 to 100 μM). At higher concentrations, the AV nodal Wenckebach cycle length and its refractory period were also prolonged (10 to 100 μM). In addition, the conduction through the His-Purkinje system (HV interval) and the atrial tissue (SA interval), as well as the spontaneous cycle length, were lengthened dose-dependently (30 to 100 μM).

4 In isolated ventricular myocytes, Na current was decreased dose-dependently by propofol. In part this was due to a negative-shift of the steady-state voltage-dependent inactivation and a slowed rate of recovery from inactivation. The I_{Na} suppression by propofol was frequency-dependent. Propofol also blocked the I_{Ca}. The ED_{50} for peak current inhibition was 6.9 ± 0.9 ($n=6$) and 8.3 ± 1.5 μM ($n=7$) for I_{Na} and I_{Ca}, respectively.

5 The transient outward potassium current (I_{to}) of atrial myocytes was suppressed with an ED_{50} of 5.7 ± 0.8 μM ($n=11$), which was only partly caused by a left-shift of the steady-state inactivation. The inward rectifier K current (I_{K1}) of the ventricular cells was reduced somewhat by propofol.

6 In summary, propofol can cause direct dromotropic and chronotropic effects on the cardiac conduction system, especially the atrioventricular node. These changes can be attributed, at least in part, to its direct dose-dependent suppression of the cardiac I_{Ca}, I_{Na} and I_{to}. Special concerns in the use of propofol anaesthesia for cardiac patients and the therapeutic antiarrythmic potential of propofol-like compounds are addressed.

Keywords: Propofol; heart conduction system; ion channel

Introduction

Propofol (2,6-diisopropylphenyl), a short acting general anaesthetic agent used for induction of anaesthesia before surgery and for sedation in intensive care unit, has been suggested for use as an anaesthetic during electrophysiological studies and ablation (Shafer *et al*., 1988; Lebovic *et al*., 1992; Smith *et al*., 1994). However, propofol has been associated with the conversion of supraventricular tachycardia into normal sinus rhythm (Hermann & Vettermann, 1992). Although this can be attributed to the indirect effects of propofol, i.e., modulation of autonomic nervous system tone and alteration of the baroreceptor reflex sensitivity, direct effects of propofol which could influence conduction have been observed on cardiac tissues (Cullen *et al*., 1987; Sellgren *et al*., 1992; Ebert & Muzi, 1994). In guinea-pig, propofol prolonged the atrioventricular (AV) conduction (or stimulus-to-His interval in paced rhythm) and the Wenckebach cycle length in a concentration-dependent manner (Alphin *et al*., 1995). Nonetheless, the underlying ionic mechanism(s) for these direct electrophysiological effects of propofol remain ill-defined. This study, by using isolated Langendorff perfused, autonomic blocked, rabbit hearts and rabbit isolated atrial and ventricular myocytes, demonstrated direct actions of propofol on the cardiac conduction system as well as the cardiac ionic currents. This systemic approach may help to define the clinical usage of propofol for cardiac anaesthesia. The therapeutic potential of propofol or related drugs for cardiac arrythmia control needs further investigation, perhaps including structure-activity data.

[1]Author for correspondence at: Department of Pediatrics, National Taiwan University Hospital, No. 7 Chung-Shen South Road, Taipei, Taiwan, 100.

Methods

New Zealand white rabbits were anaesthetized by an intravenous injection of sodium pentobarbitone (30 mg kg^{-1}, i.v.) and heparin (300 u kg^{-1}).

Intracardiac electrocardiogram recording

Animal preparation Heart was excised via thoracotomy and the aorta was retrogradely perfused (Wu *et al*., 1994a). For His bundle electrogram recording, a silver electrode connected to a tungsten spring was placed on the endocardium near the apex of the triangle of Koch to record the His bundle electrogram. In order to obtain a recognizable T wave and a ventricular depolarization simultaneously on the ventricular electrogram, the tips of the ventricular recording electrode were separated and placed on opposite sides of the ventricular epicardium near the ventricular apex. High right atrial pacing electrode was placed near the junction of the superior vena cava and right atrium. The ventricular pacing electrode was placed on the pericardium near the right ventricular apex. Pacing studies were performed by utilizing a programmable stimulator (Bloom Ltd, DTU 215). A pacing stimulus of 1 ms in duration and three times the diastolic threshold voltage was applied to the preparation through the bipolar atrial or ventricular electrodes. The signals were continuously monitored on an oscil-

loscope (Hewlett Packard, 54503A) and pertinent data recorded on a two-channel physiological recorder (Gould, RS 3200) with a paper speed of 100 mm s^{-1}.

Experimental protocol To ensure complete autonomic blockade, 1 μM atenolol and 1 μM atropine were concomitantly added to all the test solutions (control, propofol and wash solutions) and 30 min were allowed before electrophysiological measurements were made. The protocol used for electrophysiological studies was performed according to standard methods (Josephson & Seides, 1993). The average of 4 stable cycle lengths of spontaneous heart beats was taken as the parameter of the pacemaker automaticity, which could be a sinus or an atrial pacemaker. Corrected QT interval (corrected by the square root of the QT interval) was used as the parameter for monitoring ventricular repolarization. The right atrium was then paced at a constant rate which was slightly faster than the spontaneous heart rate. At this constant rate pacing, the intra-atrial conduction time (SA), AV nodal conduction time (AH) and His-Purkinje conduction time (HV) were measured.

Incremental right atrial pacing was used to determine the Wenckebach cycle length. Atrial extra-stimulation (S_1S_2) was performed to obtain the refractory periods of atrial, atrioventricular and His-Purkinje system. The ventricular effective refractory period (VERP) was also measured by use of a ventricular extrastimulation study protocol.

Solutions Tyrode solution contained (in mM); NaCl 120.3, NaH_2PO_4 1.2, $NaHCO_3$ 24.2, KCl 5, $MgCl_2$ 1.1, $CaCl_2$ 1.8, dextrose 11, which was saturated with 95% O_2 and 5% CO_2 to give a pH of 7.4 and warmed to 37°C.

Whole-cell voltage clamp recording

Cardiac atrial and ventricular myocytes were isolated as described previously (Wu *et al*., 1994b). The ionic currents were studied in whole-cell configuration at room temperature (25–27°C) (Hamill *et al*., 1981). A Dagan 8900 patch/whole cell clamp fitted with 0.1 GΩ feedback resistor in the headstage was used in the voltage clamp experiments. The total series resistance (R_s) for the pathway between the pipette interior and the cell membrane in the whole-cell configuration was calculated from the estimates of cell capacitance (C_m) and the time constant of the capacitative current decay (τ_c) from the equation $\tau_c = R_s \times C_m$. Values of the C_m were estimated from integration of capacitative current transients and had the mean ± s.e. values of 82 ± 4 pF ($n = 6$). Mean τ_c values were 109 ± 5 μs. The mean R_s for the pathway between the pipette and the cell membrane after rupture of the membrane seal was calculated to be 1.32 ± 0.05 MΩ. It was possible to compensate electronically for 60% of the voltage drop across the electrode produced by the current flow. To lower the maximal amplitude

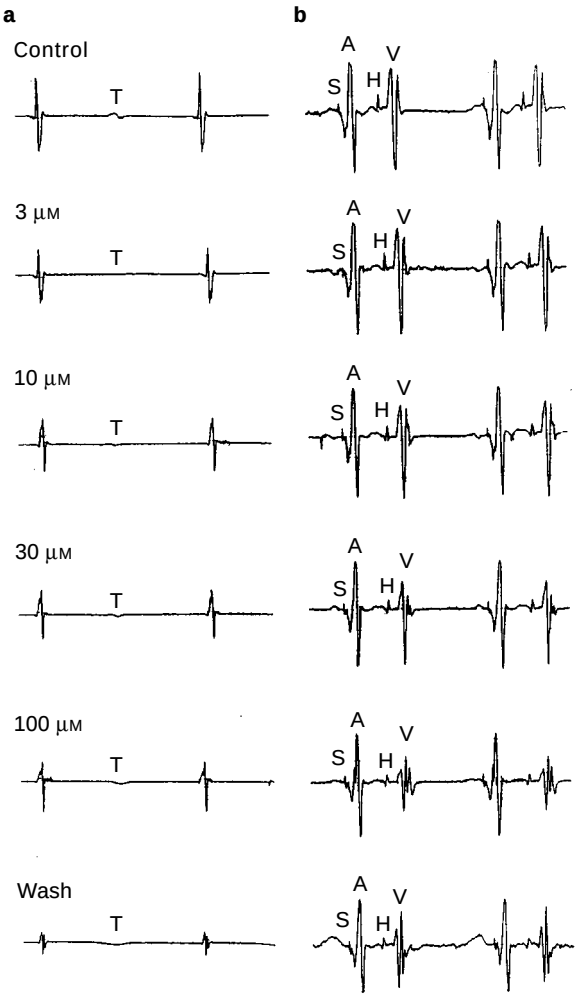

Figure 1 Representative His bundle electrogram (b) and ventricular electrogram (a) after different concentrations of propofol in the rabbit heart. The paper speed was 100 mm s^{-1}. A: atrial activity, H: His potential, S: electrical stimulation, T: T wave, V: ventricular activity.

Table 1 Changes in the electrophysiological parameters of the cardiac conduction system in rabbits induced by propofol

		Propofol (μM)				
	Control	*3*	*10*	*30*	*100*	*Wash*
BCL	435 ± 12 ($n = 8$)	440 ± 11	462 ± 9	473 ± 11*	478 ± 16*	459 ± 15
QT_c	367 ± 10	362 ± 6	347 ± 8	332 ± 6*	NA	350 ± 10
WCL	215 ± 4	235 ± 9	258 ± 9*	265 ± 16*	261 ± 12*	204 ± 5
SA	14 ± 1	14 ± 1	14 ± 2	16 ± 2*	19 ± 2*	14 ± 2
AH	51 ± 4	55 ± 5*	59 ± 6*	65 ± 5*	66 ± 5*	51 ± 5
HV	23 ± 1	23 ± 1	24 ± 1	27 ± 2*	30 ± 2*	23 ± 1
AERP	117 ± 9	112 ± 9	101 ± 10	113 ± 9	118 ± 8	112 ± 9
AVNERP	158 ± 6 ($n = 8$)	165 ± 10	178 ± 11*	193 ± 20*	188 ± 16*	150 ± 7
HPFRP	222 ± 5	230 ± 6	241 ± 6	249 ± 10	245 ± 14	226 ± 6
VERP	193 ± 10	191 ± 10	191 ± 12	186 ± 11	187 ± 14	180 ± 12

Data (in ms) were obtained from 10 experiments and are expressed as mean ± s.e. Numbers in parentheses indicate the number of experimental measurements for the parameters (BCL and AVERP) which sometimes were limited by the physiological properties. *$P < 0.05$. Abbreviations: AERP: atrial effective refractory period; AH: atrio-His bundle conduction interval; AVNERP: atrioventricular nodal effective refractory period; BCL: basic cycle length; HPFRP: His-Purkinje system functional refractory period; HV: His-ventricular conduction interval; QT_c: corrected QT interval; SA: sinoatrial conduction interval; VERP: ventricular effective refractory period; WCL: Wenckebach cycle length.

of Na currents, I_{Na} was studied in a low Na^+ Tyrode solution ($[Na^+]=54$ mM, with NaCl replaced by N-methyl-D-glucamine) and dialysis of the cell with Na-containing (10 mM) Cs^+ pipette solution. Results from experiments in which the estimated voltage error attributed to uncompensated R_s ($R_s \times I_{Na}$) was less than 5 mV were retained. Cells were exposed to each concentration of propofol for 5 min.

Solutions Three basic solutions were used with the following compositions in mM: (1) Ca^{2+}-Tyrode: NaCl 137, KCl 5.4, $MgCl_2$ 1.1, $CaCl_2$ 1.8, HEPES 12, titrated with NaOH to pH 7.4. (2) Internal solution for filling the suction pipettes: KCl 120, NaCl 10, MgATP 5, K_2 EGTA 10, $CaCl_2$ 1.5, HEPES 10, pCa, 6.8, titrated with KOH to pH 7.4. Internal solution containing 120 mM Cs^+ instead of K^+ was used for I_{Na} and I_{Ca} studies. Junction potentials of both types of pipettes were about 5–10 mV. (3) Kruftbrühe (KB) medium: taurine 10, glutamic acid 70, KCl 25, KH_2PO_4 10, dextrose 22, EGTA 0.5, titrated with KOH to pH 7.3.

Drugs Pure propofol in liquid form was a gift from ZENECA Pharmaceutical company. It was diluted in dimethysulphoxide (DMSO) as a 50 mM stock solution from which the test solutions in concentrations of 3, 10, 30 and 100 μM were prepared. Drugs were administered in a cumulative manner. No significant changes in cardiac conduction and ionic currents were shown after administration of a DMSO concentration equivalent to the amount added with 100 μM propofol.

Statistics

The data are expressed as mean $\pm$ 1 s.e. for each parameter. A repeated-measures analysis of variance followed by the Tukey test was used to examine the significance of changes after the drug. Since the drug was added in cumulative manner, only the significance ($P<0.05$) between the control and the experimental values at each concentration was indicated by asterisks.

Results

Modification of conduction system

Changes in the electrophysiological parameters of the cardiac conduction system in 10 rabbits after propofol are summarized in Table 1. Figure 1 shows an example of an intracardiac electrogram after propofol. The AH interval was significantly lengthened by propofol even at a low concentration (3 μM) and this effect was dose-dependent (3 to 100 μM). At higher concentrations, the AV nodal Wenckebach cycle length was prolonged (10 μM). The conduction through the His-Purkinje system (HV interval) and the atrial tissue (SA interval) as well as the spontaneous cycle length were also prolonged (30 μM). The corrected QT interval was decreased (30 μM).

Propofol prolonged the AV nodal refractory period at a concentration of 10 μM or higher. In the present experimental protocol (with the concomitant addition of 1 μM atenolol and 1 μM atropine) the AV node usually became refractory to premature extrastimulation before the His-Purkinje system became refractory. Therefore, only the functional refractory period of the His-Purkinje system (shortest V_1V_2 conducted) was measured. It was not signficantly changed by propofol. Neither was the refractoriness of the atrial and the ventricular tissue significantly altered by propofol.

Ionic current modification

From a holding potential of -80 mV, I_{Na} was elicited by depolarizing pulses to potentials ranging from -60 to 0 mV. Under control condition, I_{Na} was activated at the threshold potential of around -60 mV and attained its maximum around -30 mV. Propofol blocked I_{Na} (Figures 2 to 5). The maximal Na current amplitude decreased to $70\pm5\%$, $33\pm6\%$ and $4\pm5\%$ ($n=6$) after the addition of propofol at 3, 10 and 30 μM, respectively. The ED_{50} for current inhibition was 6.9 ± 0.9 μM. Propofol appeared to block the Na current by causing a negative shift of the steady-state inactivation (Figure 3). Membrane potential of Na channel half inactivation (V_{mid})

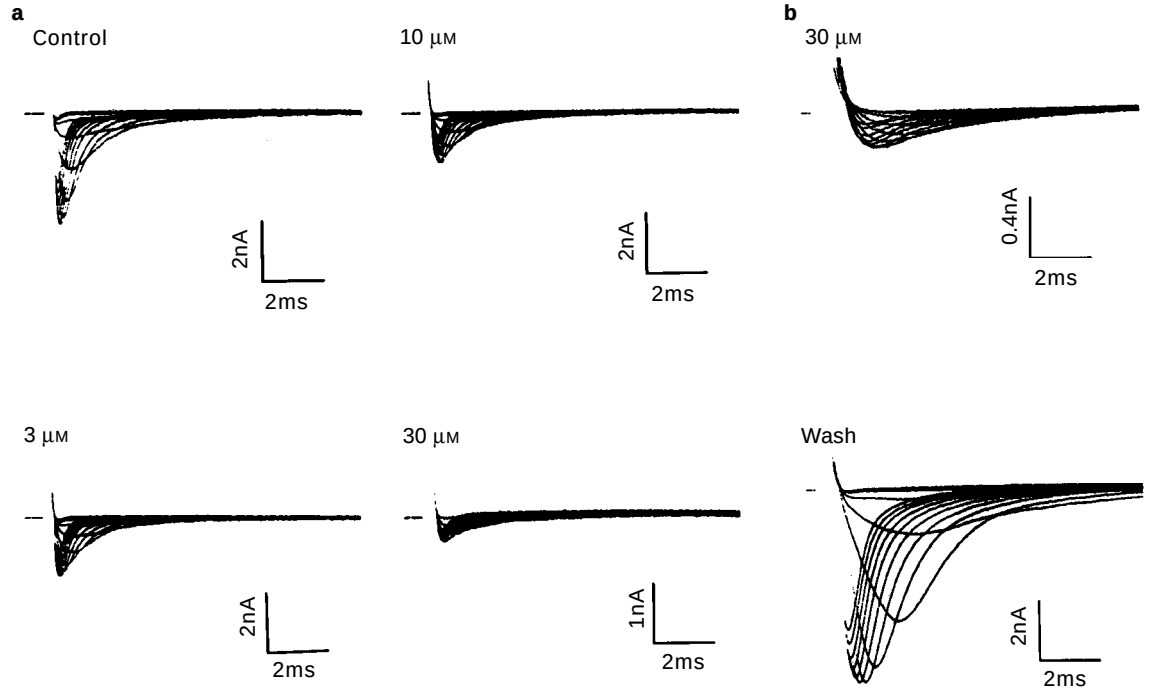

Figure 2 (a) From a holding potential of -80 mV, Na currents were serially elicited at depolarizations ranging from -60 mV to -5 mV in 5 mV steps. Propofol decreased the Na currents. (b) The suppression of I_{Na} of cells induced by 30 μM propofol and recovery of I_{Na} after wash-out of the propofol with the low Na external solution (used in the control).

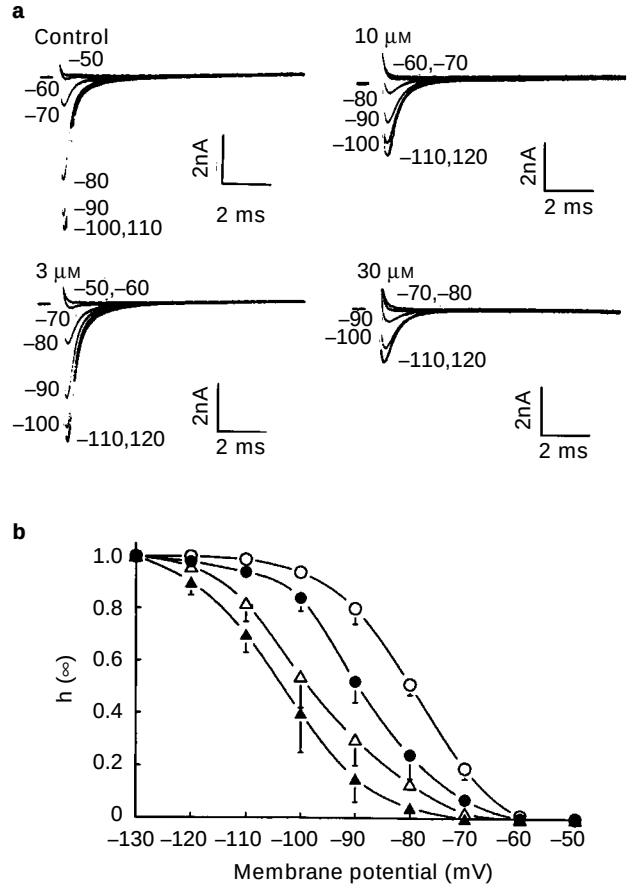

Figure 3 (a) Steady-state voltage-dependent inactivation of I_{Na} was studied by altering the holding potentials for 1 s and then applying a depolarizing pulse to −20 mV. Propofol caused a hyperpolarizing shift of the steady-state inactivation. However, the maximal current elicited on hyperpolarization after propofol was still smaller than that of control. (b) The steady-state voltage-dependent inactivation curve of I_{Na}. (○) Control; (●) 3 μM, (△) 10 μM and (▲) 30 μM propofol. Vertical lines show s.e.mean.

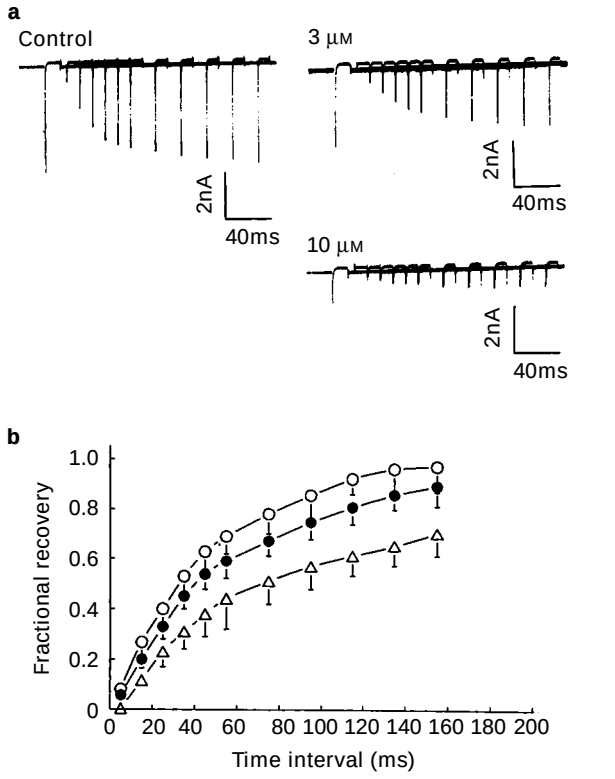

Figure 4 (a) Recovery of Na channels from inactivation. Na currents were elicited by a twin-pulse depolarization protocol. Cells were first depolarized to −20 mV for 10 ms from a holding potential of −80 mV. The kinetics of recovery were then defined by a second depolarization given at various time intervals after the first pulse. Propofol retarded the recovery of Na channels from inactivation. I_{Na} elicited after 30 μM propofol was usually very small and therefore the recovery kinetics at this concentration of propofol were not defined. (b) The recovery time course of I_{Na} from inactivation obtained from 6 cells. Ratios of the currents elicited by the second and first pulses reflected the fractions of Na channels which had recovered from inactivation. (○) Control; (●) 3 μM and (△) 10 μM propofol. Vertical lines show s.e.mean.

was obtained by curve fitting of the inactivation to the Boltzman equation. The V_{mid} was -80 ± 2, -91 ± 3, -101 ± 3 and -107 ± 5 mv ($n=8$) for the control and propofol at 3, 10 and 30 μM, respectively. With the maximum concentration of propofol (30 μM) I_{Na} elicited upon hyperpolarization was still smaller than that of control. This shows that the decrease of I_{Na} after propofol cannot be explained entirely by the negative-shift of the inactivation. Propofol also retarded the recovery of Na channel from its inactivation (Figure 4). The time constant of Na channel recovery from its inactivation was obtained from curve fitting of the recovery fraction to a single exponential function. The time constant was 55 ± 3, 78 ± 6 and 145 ± 22 ms ($n=6$) for the control and propofol at 3 and 10 μM, respectively. After 30 μM propofol, the I_{Na} elicited from a holding potential of −80 mV was very small and therefore the time constant for this concentration was not determined. The fraction of I_{Na} after propofol was plotted against different stimulation cycle length (Figure 5, $n=3$) and the relationship indicated that the suppression of I_{Na} by propofol was greater at a faster stimulation rate than at a slower one and occurred in a frequency-dependent manner.

After application of a prepulse to −40 mV to inactivate the Na and 'T'-type Ca channels, conventional L-type Ca currents were elicited at depolarized membrane potentials ranging between −30 to 40 mV in 10 mV steps. A time-dependent reduction of Ca currents ('rundown' phenomenon) was observed during the initial 10 min access of the patch pipette to the interior of the cells. Therefore, experiments were performed only on those cells with stable Ca currents 10 min after cell rupture. Propofol suppressed the L-type Ca currents (Figure 6). Peak Ca currents elicited at a potential of 0 mV were 67 ± 9, 42 ± 8 and 11 ± 7% after 3, 10 and 30 μM propofol, respectively. The ED_{50} of current inhibition was 8.3 ± 1.5 μM ($n=7$).

The delayed outward K current has been found to be extremely small in both rabbit atrial and ventricular cells (Giles & Imaizumi, 1988). Therefore, only I_{K1} and I_{to} were studied. Propofol decreased the current peak and accelerated the inactivation of I_{to} (Figure 7). The area under the current curve elicited at 60 mV represented the total charge through the I_{to} channels. The baseline of the area was obtained by rapid depolarization to fully inactivate I_{to}. The calculation by area provides a qualitative description of the changes in both the current peaks and the rate of inactivation. The integral of the I_{to} curves decreased to 62 ± 8%, 30 ± 8% and 10 ± 7% after 3, 10 and 30 μM propofol, respectively. The ED_{50} was 5.7 ± 0.8 μM ($n=11$). This inhibition of I_{to} was partly due to a left-shift of the voltage-dependent inactivation state of I_{to}. After propofol, the steady-state voltage-dependent inactivation curve of I_{to} was shifted to more negative membrane potentials (Figure 8). The membrane potential of I_{to} half-inactivation (V_{mid}) was determined by curve fitting of the inactivation to the Boltzman equation. V_{mid} was -68 ± 2, -72 ± 3, -78 ± 5 and -82 ± 5 mV ($n=6$) for the control and propofol at 3, 10 and 30 μM, respectively. After propofol treatment, I_{to} remained decreased even when large hyperpolarizing prepulses were applied. This suggests that inhibition of I_{to} by propofol is partly caused by a hyperpolarization-shift of the steady-state inactivation relationship.

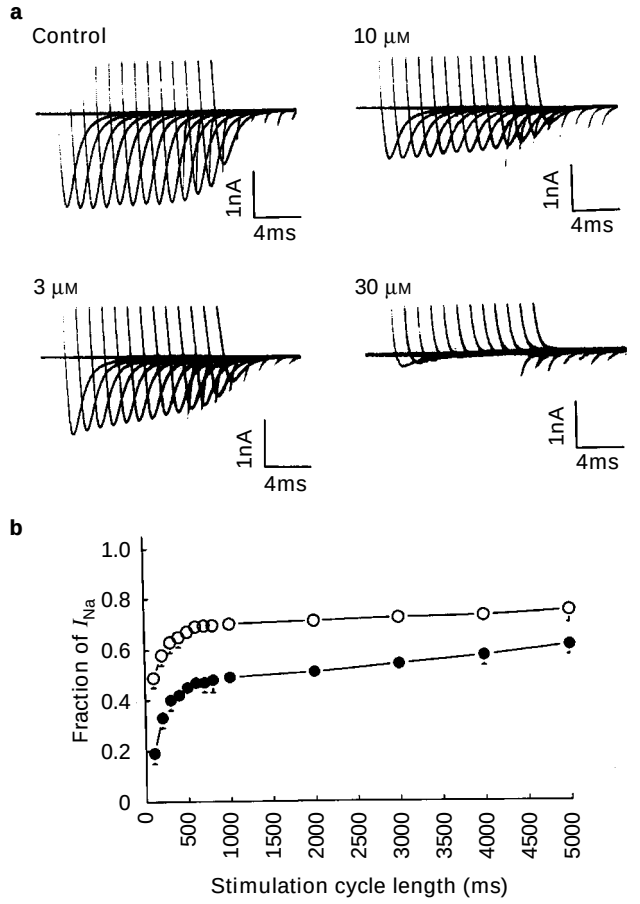

Figure 5 (a) On continuous stimulation at a constant cycle length, Na current was elicited by depolarization to −20 mV from a holding potential of −80 mV. The current traces at the 15th stimulation of each cycle length (5000, 4000, 3000, 2000, 1000, 800, 700, 600, 500, 400, 300, 200 and 100 ms) were superimposed. (b) The fraction of I_{Na} (I_{Na} after propofol/I_{Na} control) was plotted against the stimulation cycle length. The magnitude of I_{Na} suppression by propofol 3 μM (○) and 10 μM (●) was greater with the faster stimulation rate than the slower one.

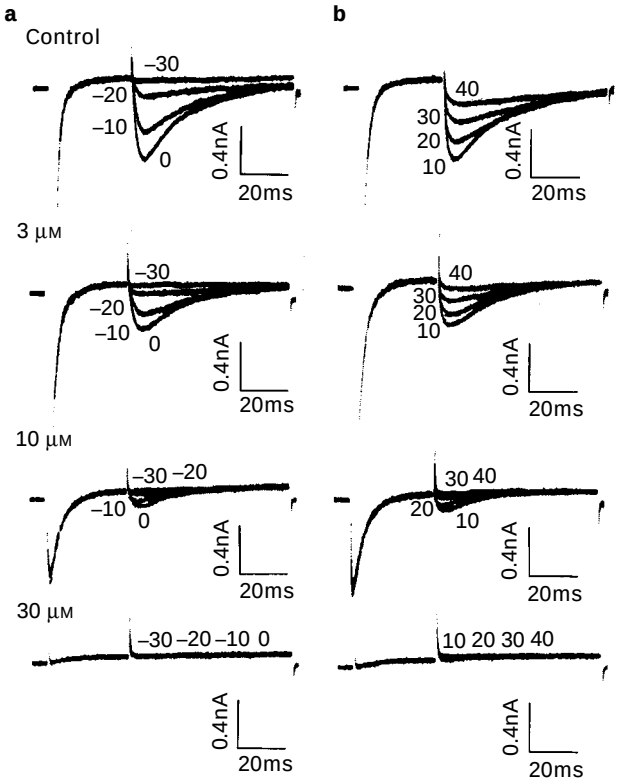

Figure 6 (a) A conditioning pulse of −40 mV was applied to inactivate the Na channel and 'T'-type Ca channels, and then a depolarizing pulse, ranging from −30 to 40 mV, of 80 ms duration was serially applied to elicit the peak L-Ca current. Propofol decreased the Ca currents in a dose-dependent manner. (b) Spontaneous rundown of the $I_{Ca\text{-}L}$ (the peak I_{Ca}) with time after rupture of the cell membrane.

I_{K1} was studied in ventricular cells pretreated with 30 μM tetrodotoxin and 1 μM cobalt to inactivate I_{Na} and I_{Ca}. Propofol also decreased I_{K1} currents but to a much lesser extent (Figure 9). The slope conductance measured between a membrane potential of −70 and −110 mV after 3, 10 and 30 μM propofol was reduced to 82±6, 75±8 and 62±9%, respectively ($n=4$). The outward hump showing the inward rectification was recorded at a voltage ranging from −50 to −30 mV and was found not to be significantly changed by propofol.

Discussion

The present study demonstrates the direct effects of propofol on the conduction system in adult rabbit hearts. Although its effects on ionic currents were measured on myocytes isolated from atrial and ventricular tissues, instead of the conduction system, the data may still provide insights into the negative dromotropic and chronotropic effects of propofol in terms of modifications of cardiac ionic channels.

In clinical anaesthesia, although the mean plasma concentration of propofol at the onset of unconsciousness after a bolus dose of 2 mg kg^{-1} may reach 10 μg ml^{-1} (56 μM), the target plasma concentration of propofol for hypnosis is defined as 2–6 μg ml^{-1} (11–34 μM) and for sedation 0.5–1.5 μg ml^{-1} (3–8 μM) (Herregods *et al*., 1987; Smith *et al*., 1994). Propofol is tightly bound to plasma protein (96–99%) (Servin *et al*., 1988; Cockshott *et al*., 1992). Therefore, the concentrations reached during clinical anaesthesia by propofol are at or below the lowest concentration of propofol evaluated in this study (3 μM). Our results showed that at such a concentration range, propofol may nevertheless retard conduction through the AV node. In guinea-pig isolated hearts, propofol prolonged the stimulus-to-His interval (an index for AV node conduction), and such prolongation could be antagonized by atropine (Alphin *et al*., 1995). Based on binding data, these negative dromotropic effects of propofol have been attributed to its actions on M_2 muscarinic receptors. However, our results obtained during conditions of autonomic blockade (isolated hearts treated with atropine 1 μM and atenolol 1 μM) still demonstrated a negative dromotropic effect of propofol on the AV node. Therefore, some other mechanism, e.g. modification of ionic channels, must be responsible for these direct electrophysiological effects of propofol.

The L-type I_{Ca} is responsible for the action potential upstroke in some regions of the rabbit AV node and consequently the density of I_{Ca} is one of the major determinants of AV nodal conduction (Kokubun *et al*., 1982; Hancox & Levi, 1994; Whalley *et al*., 1995). Based on our observations, the retarded AV nodal conduction after propofol may be due to its direct suppression of I_{Ca}. Previous studies have also shown a decrease of the transarcolemmal calcium flux after propofol and it has been proposed that this decrease is the mechanism responsible for the negative inotropy of propofol (Azuma *et al*., 1993; Cook & Housmans, 1994). In guinea-pig isolated myocytes, propofol has also been shown to alter the kinetics of the opening and closing of calcium channels (Takahashi *et al*., 1994).

In clinical anaesthesia, propofol has been associated with conversion of supraventricular tachycardia into normal sinus rhythm (Hermann & Vettermann, 1992). Transient AV con-

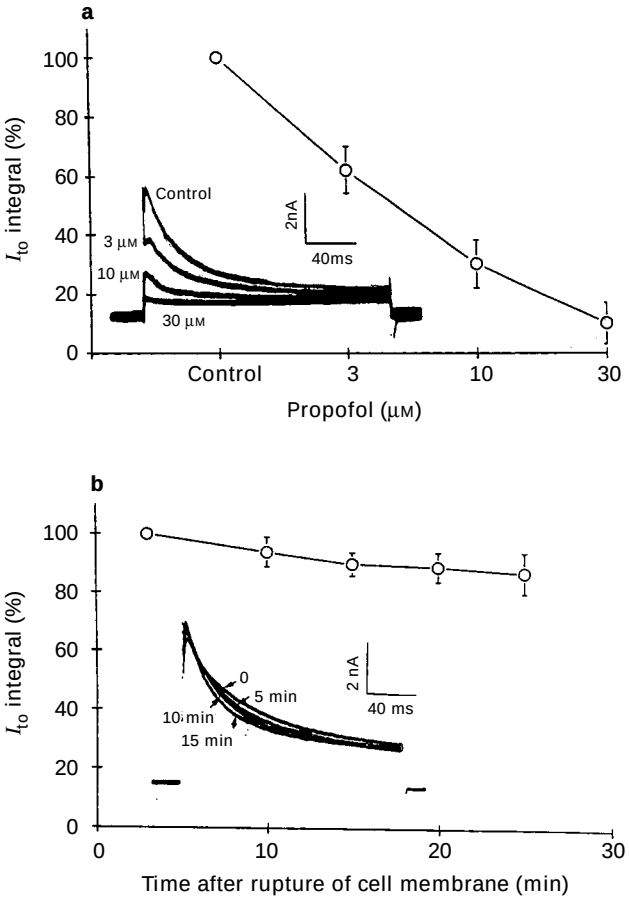

Figure 7 (a) I_{to} was studied in the presence of 0.5 mM $CoCl_2$ to eliminate the contamination of I_{Ca}. Repetitive depolarization to 60 mV from a holding potential of −80 mV at a slow stimulation frequency of 0.1 Hz was used to ensure complete recovery of these currents from their inactivation state. Propofol decreased the I_{to} peak and accelerated the inactivation. (b) Spontaneous 'rundown' phenomenon of I_{to} with time. Insert shows current traces recorded at 0, 5, 10 and 15 min after rupture of the cell membrane.

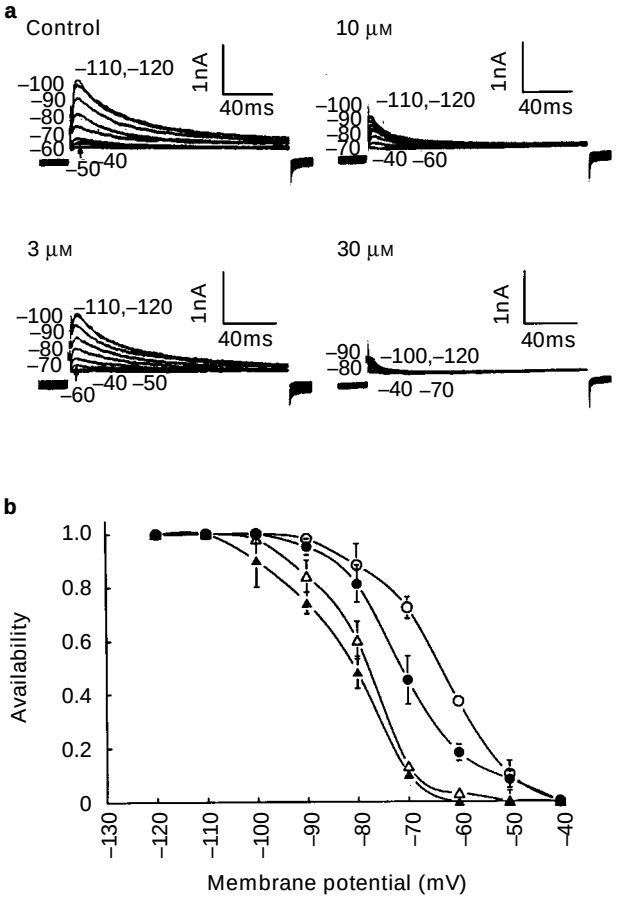

Figure 8 (a) Steady-state voltage-dependent inactivation of I_{to} was studied by altering the holding potentials for 1 s and then applying a depolarizing pulse to +60 mV at a stimulation frequency of 0.1 Hz. (b) Steady-state voltage-dependent inactivation curve of I_{to}. A small degree of negative-shift in the steady-state voltage-dependent inactivation was observed after propofol (●) 3 μM, (△) 10 μM and (▲) 30 μM. (○) Control.

duction block has also been found in patients who had received propofol as an anaesthetic (James *et al*., 1989; Ganansia *et al*., 1989). The direct suppressive effects of propofol on AV node, as demonstrated by this study, may be responsible for these phenomena. However, Sharpe *et al*. (1995) failed to find direct effects of propofol on the normal sinoatrial and AV node of Wolff-Parkinson-White patients during alfentanil/midazolam anaesthesia. The discrepancy of these clinical observations may be related to the different AV nodal vulnerabilities of the patients, different plasma concentrations, or the interaction of the combination drugs.

The threshold concentration of propofol needed to retard cardiac conduction was lowest for the AV node and this level may be reached during its clinical use. However, the conduction through the His-Purkinje system and the atrial tissue, and the spontaneous cycle length could also be slowed down at higher propofol concentrations which are rarely encountered in clinical anaesthesia. Significant lengthening of the refractory periods after propofol was found only in the AV node. Our data on the cardiac ionic currents indicated a multiple ionic mechanism for such an electrophysiological modification. Direct effects of propofol on ionic channels have been described but the number of such studies is very limited (Veintemilla *et al*., 1992; Baum, 1993). In the myelinated axon of *Xenopus laevis*, propofol caused a negative shift of the steady state inactivation curves of I_{Na} (Veintemilla *et al*., 1992). In guinea-pig isolated ventricular myocytes, propofol (28 μM) decreased the delayed rectifier K currents (Baum, 1993). Our data revealed an inhibitory role of propofol on the cardiac I_{Na}, I_{Ca} and I_{to}. Cardiac Na channel blockade is usually associated with retarded conduction and increased tissue refractoriness of the atrial, His-Purkinje system and the ventricular tissues, whereas calcium channel blockade results in similar changes in the AV nodal tissue (Wit & Granfield, 1974; Sheets *et al*., 1988; Fozzard, 1990; Whalley *et al*., 1995). As demonstrated by our data, propofol blocks the Na channel in a frequency-dependent manner which is a common feature of type I antiarrhythmic agents (Grant & Wendt, 1992). On the other hand, a decrease of I_{Ca} in atrial, His-Purkinje system and ventricular tissue may also shorten the action potential duration and subsequently the refractory periods of these tissues (Wit & Cranfield, 1974; Rosen *et al*., 1974; Whalley *et al*., 1995). We observed a retarded conduction through the AV node, His-Purkinje system and intraatrial tissue as well as a significant lengthening of AV nodal refractory period after propofol. Furthermore, I_{to}, the repolarizing current for the phase 1 repolarization, was also decreased after propofol. I_{to} inhibition may help to maintain the depolarization and slow the inactivation of I_{Ca} (Carmeliet, 1993). However, the I_{to} of rabbit myocytes undergoes voltage- and time-dependent inactivation and its channels are characteristically slow to recover from inactivation (Fermini *et al*., 1992). This behaviour may diminish its importance in early afterdepolarization as the diastolic recovery interval shortened.

In conclusion, in both control conditions and after the addition of propofol, a complex interplay of the inward and outward currents during the action potential plateau and

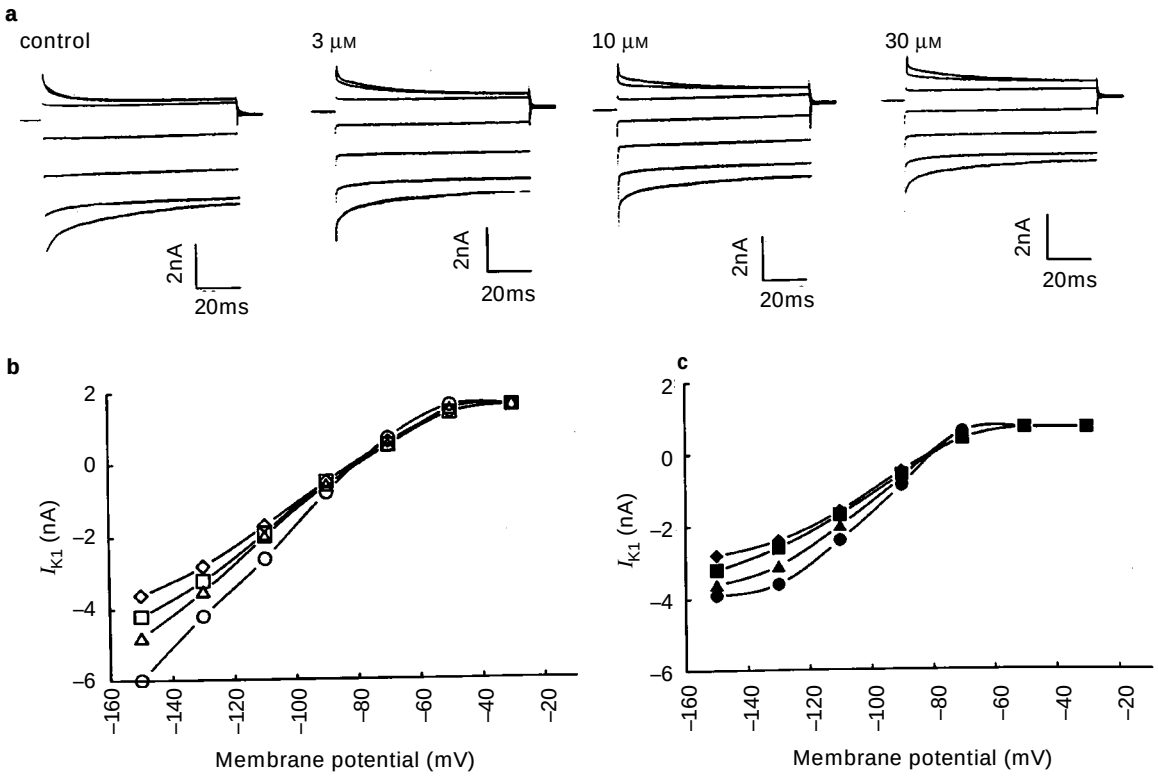

Figure 9 The steady-state current-voltage relationship of the I_{K1} after propofol. In the presence of tetrodotoxin (30 μM) to block the I_{Na} and cobalt (1 μM) to block the I_{Ca}, the I_{K1} was serially elicited from a threshold potential of -80 mV to potentials ranging from -30 to -150 mV in 20 mV steps. (a) Current traces of the I_{K1} elicited in the absence and presence of propofol. (b) The current-voltage relation of I_{K1} measured at the beginning of the current traces in the absence (○, control) and presence of propofol (△) 3 μM, (□) 10 μM and (◇) 30 μM. (c) The steady state current-voltage relation of I_{K1} in the absence (●, control) and presence of propofol (▲) 3 μM, (■) 10 μM and (◆) 30 μM. The I_{K1} currents elicited at potentials more negative than -70 mV were decreased. The outward hump (showing the inward rectification) in the range -60 to -20 mV was not significantly modified.

repolarization occurs in the cardiac myocyte. Although the voltage clamp data were not obtained from cells of the conduction system, we may still infer the modification of cardiac conduction system properties after propofol to the net effects of such interplay. Special concerns of propofol anaesthesia for cardiac patients and the therapeutic potential of propofol or related compounds for cardiac arrhythmias are suggested.

References

ALPHIN, R.S., MARTENS, J.R. & DENNIS, D.M. (1995). Frequency-dependent effects of propofol on atrioventricular nodal conduction in guinea pig isolated heart. *Anesthesiology*, **83,** 382–394.

AZUMA, M., MATSUMURA, C. & KEMMOTSU, O. (1993). Inotropic and electrophysiologic effects of propofol and thiamytal in isolated papillary muscles of the guinea pig and the rat. *Anesth. Analg.*, **77,** 557–563.

BAUM, V.C. (1993). Distinctive effects of three intravenous anesthetics on the inward rectifier (I_{K1}) and the delayed rectifier (I_K) potassium currents in myocardium: implications for the mechanism of action. *Anesth. Analg.*, **76,** 18–23.

CARMELIET, E. (1993). Mechanisms and control of repolarization. *Eur. Heart. J.*, **14** (suppl H), 3–13.

COCKSHOTT, D.I., DOUGLAS, E.J., PLUMME, G.F. & SIMONS, P.J. (1992). The pharmacokinetics of propofol in laboratory animals. *Xenobiotica*, **22,** 369–375.

COOK, D.J. & HOUSMANS, P.R. (1994). Mechanism of the negative inotropic effect of propofol in isolated ferret ventricular myocardium. *Anesthesiology*, **80,** 859–871.

CULLEN, P.M., TURTLE, M., ROBERTS-PRYS, C., WAY, W.L. & DYE, J. (1987). Effect of propofol anesthesia on baroreflex activity in humans. *Anesth. Analg.*, **66,** 1115–1120.

EBERT, T.J. & MUZI, M. (1994). Propofol and autonomic reflex function in humans. *Anesth. Analg.*, **78,** 369–375.

FERMINI, B., WANG, Z., DUAN, D. & NATTEL, S. (1992). Differences in rate dependence of transient outward current in rabbit and human atrium. *Am. J. Physiol.*, **263,** H1747–H1754.

FOZZARD, H.A. (1990). The roles of membrane potential and inward Na^+ and Ca^{2+} currents in determining conduction. In *Cardiac Electrophysiology: A Textbook*. ed. Rosen, M.R., Janse, M.J. & Wit, A.L. pp. 415–425. New York: Futura publishing Co. Inc.

GANANSIA, M.F., FRANCOIS, T.P., ORMEZZANO, X., PINAUD, M.L. & LEPAGE, J.Y. (1989). Atrioventricular Mobitz I block during propofol anesthesia for laparoscopic tubal ligation. *Anesth. Analg.*, **69,** 524–525.

GILES, W.R. & IMAIZUMI, Y. (1988). Comparison of potassium currents in rabbit atrial and ventricular cells. *J. Physiol.*, **405,** 123–145.

GRANT, A.O. & WENDT, D.J. (1992). Block and modulation of cardiac Na^+ channels by antiarrhythmic drugs, neurotransmitters and hormones. *Trends Pharmacol. Sci.*, **13,** 352–358.

HANCOX, J.C. & LEVI, A.J. (1994). L-type calcium current in rod- and spindle-shaped myocytes isolated from rabbit atrioventricular node. *Am. J. Physiol.*, **267,** H1670–1680.

HAMILL, O.P., MARTY, A., NEHER, E., SAKMANN, B. & SIGWORTH, F.J. (1981). Improved patch clamp techniques for high resolution current recording from cells and cell-free membrane patches. *Pflügers Arch.*, **391,** 85–100.

HERMANN, R. & VETTERMANN, J. (1992). Change of ectopic supraventricular tachycardia to sinus rhythm during administration of propofol. *Anesth. Analg.*, **75,** 1030–1032.

HERREGODS, L., ROLLY, G., VERSICHELEN, L. & ROSSEEL, M.T. (1987). Propofol combined with nitrous oxide-oxygen for induction and maintenance of anaesthesia. *Anaesthesia*, **42,** 360 – 365.

JAMES, M.F.M., REYNEKE, C.J. & WHIFFLER, K. (1989). Heart block following propofol: a case report. *Br. J. Anesth.*, **62,** 212 – 215.

JOSEPHSON, M.E. & SEIDES, S.F. (1993). *Clinical Cardiac Electrophysiology. Technique and Interpretations*. pp. 22 – 70. Philadelphia: Lea & Febiger.

KOKUBUN, S., NISHMURA, M. & NOMA, A. (1982). Membrane currents in rabbit atrioventricular node cell. *Pflügers Arch.*, **393,** 15 – 22.

LEBOVIC, S., REICH, D.L., STEINBERG, G., VELA, F.P. & SILVAY, G. (1992). Comparison of propofol versus ketamine for anesthesia in pediatric patients undergoing cardiac catheterization. *Anesth. Analg.*, **74,** 490 – 494.

ROSEN, M.R., ILVENTO, J.P., GELBAND, H. & MERKER, C. (1974). Effects of verapamil on electrophysiologic properties of canine cardiac Purkinje fibers. *J. Pharmacol. Exp. Ther.*, **189,** 414 – 422.

SELLGREN, J., BIBER, B., HENRIKSON, B., MARTNER, J. & PONTEN, J. (1992). The effects of propofol, methohexitone and isoflurane on the baroreceptor reflex in the cat. *Acta Anaesthesiol. Scand.*, **36,** 784 – 790.

SERVIN, F., DESMONTS, J.M., HABERER, J.P., COCKSHOTT, I.D., PLUMMER, G.F. & FARINOTI, R. (1988). Pharmacokinetics and protein binding of propofol in patients with cirrhosis. *Anesthesiology*, **59,** 887 – 891.

SHAFER, A., DOZE, V.A., SHAFER, S.L. & WHITE, P.F. (1988). Pharmacokinetics and pharmacodynamics of propofol infusion in general anesthesia. *Anesthesiology*, **69,** 348 – 356.

SHARPE, M.D., DOBKOWSKI, W.B., MURKIN, J.M., KLEIN, G. & YEE, R. (1995). Propofol has direct effect on sinoatrial node function or on normal atrioventricular and accessory pathway conduction in Wolff-Parkinson-White syndrome during alfentanil/midazolam anesthesia. *Anesthesiology*, **82,** 888 – 895.

SHEETS, M.F., HANCK, D.A. & FOZZARD, H.A. (1988). Nonlinear relationship between V_{max} and I_{NA} in canine cardiac Purkinje cells. *Circ. Res.*, **63,** 386 – 398.

SMITH, J.S., WHITE, P.F. & GOULD, R. (1994). Propofol. An update on its clinical use. *Anesthesiology*, **81,** 1005 – 1043.

TAKAHASHI, H., PUTTICK, R.M. & TERRAR, D.A. (1994). The effects of propofol and enflurane on single calcium channel currents of guinea-pig isolated ventricular myocytes. *Br. J. Pharmacol.*, **111,** 1147 – 1153.

VEINTEMILLA, F., ELINDER, F. & ARHEM, P. (1992). Mechanisms of propofol action on ion currents in the myelinated axon of xenopus laevis. *Eur. J. Pharmacol.*, **218,** 59 – 68.

WHALLEY, D.W., WENDT, D.J. & GRANT, A.O. (1995). Basic concepts in cellular cardiac electrophysiology. part I: Ion channels, membrane currents, and the action potential. *Pacing and Clinical Electrophysiology*, **18,** 1556 – 1574.

WIT, A.L. & CRANFIELD, P.F. (1974). Effect of verapamil on the sinoatrial and atrioventricular nodes of the rabbit and the mechanism by which it arrests reentrant atrioventricular nodal tachycardia. *Circ. Res.*, **35,** 413 – 425.

WU, M.H., SU, M.J., LEE, S.S. & YOUNG, M.L. (1994a). The electrophysiological effects of antiarrhythmic potential of a secoaporphine, N-allylsecoboldine. *Br. J. Pharmacol.*, **113,** 221 – 227.

WU, M.H., SU, M.J. & LUE, H.C. (1994b). Age-related quinidine effects on ionic currents of rabbit cardiac myocytes. *J. Mol. Cell. Cardiol.*, **26,** 1167 – 1177.

(Received November 29, 1996
Revised February 7, 1997
Accepted February 24, 1997)